Photoinduced Electron Transfer Occurs between 2-Aminopurine and the DNA Nucleic Acid Monophosphates: Results from Cyclic Voltammetry and Fluorescence Quenching

ARTICLE *in* THE JOURNAL OF PHYSICAL CHEMISTRY B · AUGUST 2010

Impact Factor: 3.3 · DOI: 10.1021/jp102355v · Source: PubMed

4 AUTHORS, INCLUDING:

Madhavan Narayanan
University of Pennsylvania
9 PUBLICATIONS **59** CITATIONS
SEE PROFILE

Goutham Kodali
University of Pennsylvania
30 PUBLICATIONS **152** CITATIONS
SEE PROFILE

Robert J Stanley
Temple University
47 PUBLICATIONS **963** CITATIONS
SEE PROFILE

Photoinduced Electron Transfer Occurs between 2-Aminopurine and the DNA Nucleic Acid Monophosphates: Results from Cyclic Voltammetry and Fluorescence Quenching

Madhavan Narayanan, Goutham Kodali, Yangjun Xing, and Robert J. Stanley*

Department of Chemistry, Temple University, Philadelphia, Pennsylvania 19122

Received: March 15, 2010; Revised Manuscript Received: May 7, 2010

2-Aminopurine (2AP) is a fluorescent adenine analogue that is useful in part because its substantial fluorescence quantum yield is sensitive to base stacking with native bases in ss- and ds-DNA. However, the degree of quenching is sequence dependent and the mechanism of quenching is still a matter of some debate. Here we show that the most likely quenching mechanism in aqueous solution involves photoinduced electron transfer (PET), as revealed by cyclic voltammetry (CV) performed in aprotic organic solvents. These potentials were used with spectroscopic data to obtain excited-state reduction and oxidation potentials. Stern−Volmer (S−V) experiments using the native base monophosphate nucleotides (NMPs) rGMP, rAMP, rCMP, and dTMP were performed in aqueous solution to obtain quenching rate constants k_q. The results suggest that 2AP* can act as either an electron donor or an electron acceptor depending on the particular NMP but that PET proceeds for all NMPs tested.

Introduction

Understanding the structure and dynamics of nucleic acids is a prerequisite toward elucidating such basic biological processes as replication, transcription, and DNA repair. Optical spectroscopy is a noninvasive technique that is useful in detecting and monitoring structure and dynamics. The natural bases (NBs) adenine, guanine, cytosine, and thymine found in DNA (and uracil in RNA) have substantial extinction coefficients in the near-ultraviolet centered around 260 nm. Changes in these extinction coefficients resulting from the interaction of the individual transition dipole moments of the bases (i.e., hypochromism[1]) have been exploited to measure the overall stability of DNA, and much of what we know about the thermodynamics of DNA and RNA stability has been gleaned from UV spectroscopy.[2] However, the overlap of the base spectra has limited the application of this technique to studying the properties of specific sequences in any systems consisting of more than about 10 bases. Fluorescence spectroscopy is another potentially valuable noninvasive approach, but the native bases have been long recognized as nonfluorescent,[3–8] probably due to the presence of conical intersections on the excited-state potential energy surface away from the Franck−Condon region.[9–11]

In 1969 Ward, Reich, and Styrer published their seminal work on the fluorescent properties of 2-aminopurine (2AP; see Scheme 1), the 2-amino analogue of adenine (6-aminopurine).[12] Changing the position of the amino group altered the electronic properties of the molecule, resulting in a red-shifted absorption and a spectacular increase in the fluorescence quantum yield of the analogue while preserving the ability of the fluorescent base analogue (FBA) to engage in Watson−Crick base pairing. The absorption spectrum of 2AP shifted to about 305 nm, well to the red of the native base absorption. This provides for selective excitation of the analogue and has been well characterized.[13–15] Most importantly, the substantial quantum yield of 2AP was found to be sensitive to base stacking.[13–18] This feature has been exploited by many workers to afford a dynamic probe of changes in DNA structure induced by environmental factors or by proteins that modify or repair DNA.[19–28]

SCHEME 1: Chemical Structure of 2AP Used in This Study

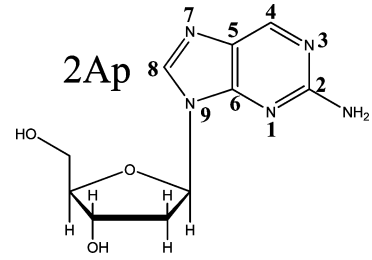

To fully exploit the data obtained from these studies, it is critical to have a clear picture of how the emission quantum yield varies according to both structure and sequence. Studies on 2AP complexed with the NBs and in oligonucleotides suggest that photoinduced electron transfer (PET) is the predominant quenching pathway. Most of the evidence for this conclusion comes from time-resolved spectroscopy, although not all groups agree with this interpretation of the data.[29–31] Data from steady-state quenching methods (e.g., the Stern−Volmer method[32–34]) have also provided important evidence supporting the PET mechanism, but pulse radiolysis experiments of 2AP:GMP mixtures suggest that quenching might occur through Dexter energy transfer.[35]

Quenching by PET can afford a very sensitive measure of structural changes due to the exponential dependence of donor−acceptor distance on the electron transfer rate.[36] However, the sequence specificity of quenching is modulated by the driving force for this reaction and hence by the redox potentials of the reactants. These, in turn, determine the direction of electron transfer and afford an assignment of the excited-state FBA as an electron donor or acceptor. In the case of 2AP*, only the oxidation potential of the ground state has been measured electrochemically[37] while the excited-state reduction

* To whom correspondence should be addressed. E-mail: rstanley@temple.edu.

10.1021/jp102355v
Published on Web 07/27/2010

potential has been estimated using ultrafast spectroscopy and the Marcus relation.[29,34] Here we present, for the first time we believe, a thorough examination of the electrochemistry of 2AP in aprotic organic solvents and apply these results to the aqueous case to show that 2AP* undergoes quenching by PET as both a donor and an acceptor.

The classic approach to obtaining excited-state potentials is to perform Stern−Volmer (S−V) quenching experiments[38] to obtain the quenching rate constant k_q (eq 1a):

$$\frac{I_0}{I} = 1 + k_q\tau_0[Q] \tag{1a}$$

$$\frac{I_0}{I} = B + (K_S + K_d)[Q] + K_SK_d[Q]^2 \tag{1b}$$

The S−V model assumes that quenching occurs only through collisions with the quencher Q with an excited-state donor

$$D^* + Q \xrightarrow{k_q} D + Q$$

and that k_q is the bimolecular rate constant for this deactivation process. A modified form of the S−V equation takes into account static quenching (eq 1b), in which case the equilibrium constant for complex formation, $K_S = [DQ]/[D][Q]$, and the constant for dynamic quenching, $K_d = \tau_0 k_q$, are separated. Here, the intercept, B, usually unity, is included because of evidence of instrumental error at very low concentrations of quencher (vide infra).

If the FBA excited-state lifetime, τ_0, is known, then $k_q = K_d/\tau_0$. These k_q values can be related to the rate constant of photoinduced electron transfer k_{ET} through the free and reorganization energies for this process, along with some estimates about the properties of the donor−acceptor complex. ΔG°_{ET} for the photoinduced electron transfer can be calculated using the Rehm−Weller equation.[39] This approach requires knowledge of the excited-state reduction and oxidation potentials of 2AP*. These excited-state reduction and oxidation potentials were obtained using the $S_0 \rightarrow S_1$ transition energy, E_{00}, and the ground-state reduction and oxidation potentials,[40] which we have measured by cyclic voltammetry (vide infra) in aprotic organic solvents. An important advantage to obtaining these values in aprotic organic solvent is that proton transfer from the solvent is not possible, simplifying the interpretation of the voltammograms. As has been shown by Seidel et al. in the case of the native bases, redox potentials obtained in aprotic organic solvents can be extrapolated to corresponding potentials in aqueous solution. This usually involves applying a potential shift in the range of −0.1 to −1.0 V, depending on the reorganization energy.[40,41] Once this information is in hand, it is possible to determine whether the FBA* can act as a donor or an acceptor in the PET reaction.

Materials and Methods

Guanosine monophosphate (ribose form, rGMP), adenosine monophosphate (rAMP), cytidine monophosphate (rCMP), deoxythymidine monophosphate (dTMP), 2-aminopurine free base (2AP; all purchased from Sigma Aldrich), and deoxyribose-2-aminopurine (d2AP, Berry and Associates) were used as received for fluorescence quenching and cyclic voltammetry (CV) experiments. HPLC-grade acetonitrile (ACN) from ACROS and HPLC-grade water from Fisher Scientific were used for this purpose.

The concentrations of the samples for fluorescence experiments were determined in 0.1 M potassium phosphate buffer, pH 7.0, by UV/vis absorption spectroscopy using an HP8452A diode array spectrophotometer. The following extinction coefficients were used: rGMP, $\varepsilon_{260} = 12\,080\ M^{-1}\ cm^{-1}$; [42] rAMP, $\varepsilon_{260} = 15\,020\ M^{-1}\ cm^{-1}$;[42] rCMP, $\varepsilon_{260} = 7070\ M^{-1}\ cm^{-1}$;[42] dTMP, $\varepsilon_{260} = 8560\ M^{-1}\ cm^{-1}$;[42] and 2AP, $\varepsilon_{317} = 6000\ M^{-1}\ cm^{-1}$.[43]

The steady-state fluorescence of the 2AP:NMP pairs was measured using a Horiba Jobin Yvon Fluoromax-2 fluorimeter at 20 °C, with a fixed concentration of 2AP (20 μM) while varying the NMP concentrations from 0.01 to 50.0 mM. A septum-sealable thermostated quartz cuvette was used. The cuvette had four optical windows and internal dimensions of 0.4 × 1.0 cm. All samples were equilibrated at 20 °C for 15 min before each measurement. Excitation was performed at 325 nm through the 0.4 cm path, and emission was collected at 90°. The excitation and emission slits were 1 and 4 nm, respectively. Scans were taken with a 2 nm step size using an integration time of 0.1 s/point. The integrated fluorescence from an average of five consecutive scans was used for the S−V analyses. The wavelength range was 330−650 nm. Plots of I_0/I vs [NMP] were fitted using Origin 7.0 (OriginLab) to obtain the K_S, K_d, and B values. The R^2 values obtained from these fits were at least 0.99.

CV measurements were performed at 20 °C on 1.0 mM solutions of d2AP using a CH610C electrochemical analyzer (CH Instruments, Inc., Texas). The redox potentials were measured in two electrolyte systems: 0.1 M *tert*-butyl ammonium hexafluorophosphate (TBAF, Fluka) dissolved in dry distilled ACN or dry distilled *N*,*N*-dimethylformamide (DMF). These two electrolyte systems were used to cover two different voltage ranges: 0.1 M TBAF/ACN was useful from −2.17 to +1.83 V vs normal hydrogen electrode (NHE) and 0.1 M TBAF/DMF was useful from −2.71 to +1.37 V vs NHE. TBAF was dried at 50 °C for 10−12 h to remove any residual water. A small homemade glass sample cell was used to accommodate sample volumes of 300−1000 μL and the three electrodes. The electrode setup consisted of a glassy carbon working electrode, a Pt wire counter electrode, and an Ag wire dipped in 10 mM $AgNO_3$ in ACN, which served as the nonaqueous reference electrode. All the samples were purged for 5 min with Ar before the scan. A gentle stream of Ar above the cell was used to maintain the solutions in an anoxic/anhydrous state during the acquisition of all scans. To calibrate the system, the $E_p^{1/2}$ of 1.0 mM ferrocene in the respective electrolytes was used as a reference for voltages measured against the nonaqueous Ag^+/Ag reference electrode to the NHE. The $E_p^{1/2}$ of 1.0 mM ferrocene was 80 ± 8 mV in ACN/0.1 M TBAF and 83 ± 11 mV in DMF/0.1 M TBAF against nonaqueous Ag^+/Ag electrode (data not shown). The shift to the NHE was calculated based on the $E_p^{1/2}$ reported in the literature for ferrocene against NHE.[44]

Theoretical one electron redox potentials of 9-methyl-2AP were calculated using density functional theory (DFT) on the methylated form using Gaussian 03.[45] 9-Methyl-2AP was used instead of the nucleoside in order to reduce computational time. A polarizable continuum model (PCM) was used to calculate redox potentials in ACN and DMF. The structures of 2AP were first optimized in vacuo at the Hartree−Fock level of theory followed by DFT using a B3LYP functional and 6-31G(d,p), 6-31++G(d,p), and 6-311+G(2d,2p) basis sets. This optimized structure was used as the initial geometry for calculations in

TABLE 1: Fluorescence Quenching Constant, $k_q = K_d/\tau_0$, of 2AP* against Various Nucleotide Quenchers As Derived from Fitting the I_0/I vs [Q] Data Using the Modified Stern−Volmer Equation (1b)[a,b]

NMP	B (±0.01)	K_d (±σ) (M^{-1})	K_S (±σ) (M^{-1})	$k_q \times 10^{-9}$ (±σ) (M^{-1} s^{-1})
G	1.00	28.66 (3.50)	1.43 (1.63)	2.52 (0.72)
A	1.01	17.60 (1.45)	4.96 (0.99)	1.55 (0.42)
C	1.00	16.20 (2.01)	0.16 (1.16)	1.43 (0.41)
dT	1.00	19.41 (0.64)	2.21 (0.37)	1.71 (0.44)

[a] The fitting error in k_q is given in parentheses. K_S represents the equilibrium constant for ground-state complexation, and B is the fitted y-intercept. [b] Several values are reported in the literature for the lifetime of 2AP.[31,34,50,55,59] We have used 11.4 (±2.9) ns as an average (and error) of these values.

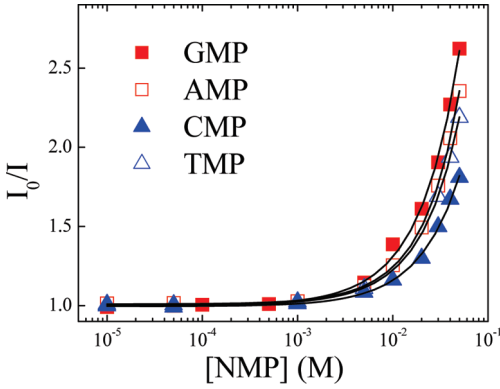

Figure 1. S−V plots for 2AP* quenched by rGMP, rAMP, rCMP, and dTMP. All fluorescence quenching measurements were made in potassium phosphate buffer, pH 7.0, at 20 °C. The solid black lines are fits to the data using the modified Stern−Volmer equation (see eq 1b). The fit parameters are tabulated in Table 1.

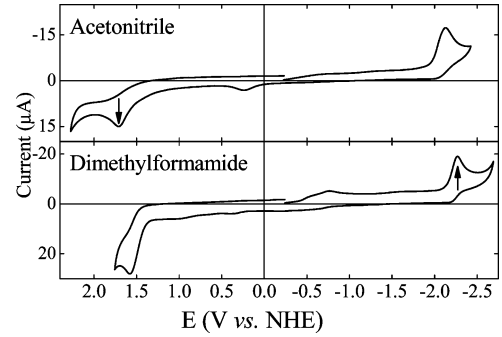

Figure 2. CVs of 2AP in ACN/0.1 M TBAF (left) and in DMF/0.1 M TBAF (right). A 100 mV/s scan rate was used for these scans. All scans were initiated in the negative scan direction. The arrows indicate the oxidation and reduction peaks used in the calculation of the excited-state redox potentials.

ACN ($\varepsilon = 35.9$) and DMF ($\varepsilon = 36.7$)[46] using the PCM[47–49] and were analyzed carefully to make sure none had imaginary frequencies. More details about these calculated potentials, including estimates of the neutral, radical cation, and anion energies in a PCM "solvent" can be found in Table S.1 in the Supporting Information.

Results

Modified Stern−Volmer Analysis of Steady-State Emission Quenching. The integrated steady-state fluorescence intensities for 2AP*:NMP pairs were fitted to the modified Stern−Volmer equation (eq 1b) to obtain K_S, K_d, and B values, as summarized in Table 1, This intercept was only a few percent from 1.00 for all NMPs. k_q can be obtained from K_d as described above if τ_0 is known. Several values are reported in the literature for the (monoexponential) lifetime of 2AP.[31,34,50] We have used 11.4 ns as an average of these values.

The fluorescence quenching experiments on 2AP* (Figure 1) show that both purine monophosphates (■, rGMP; □, rAMP) and pyrimidine monophosphates (▲, rCMP; △, dTMP) quench with comparable efficiency. The order of quenching, based on k_q, is rGMP > dTMP ~ rAMP ~ rCMP. rAMP appears to form complexes more readily with 2AP than the other NMPs with $K_S \sim 5$ M^{-1}. We observed that 2AP* was also quenched significantly by rGTP and rATP in phosphate buffer ($k_q = 2.8 \times 10^9$ and 3.2×10^9 M^{-1} s^{-1}, respectively, based on eq 1a, data not shown). The differences between our observations and those from other reports[32,34] are discussed below. We also measured the fluorescence of 2AP* in DMF with adenosine and guanosine (only the nucleosides were sufficiently soluble in DMF) and found that neither of them was an effective quencher (data not shown). This clearly indicates the important role played by solvation, which is discussed more fully below.

The enhanced quenching of purines appears to marginalize the significance of Watson−Crick (WC) base pairing in complex formation. If base pairs were stabilized through WC hydrogen bonding, then we would expect to see this effect in the k_q for 2AP* with T. No evidence for this hypothesis is found, perhaps because complexes formed via WC base pairing might not undergo quenching because there is no overlap of the relevant orbitals for electron transfer. Given that the solvent is water, there is no significant energetic advantage for WC complexes to form.

Cyclic Voltammetry (CV) of 2AP. CV measurements were performed on 2AP in two electrolyte systems as described above (see Figure 2). Since only ACN could provide a high enough positive potential, E°_{OX} values were obtained in that solvent. E°_{RED} values measured in DMF were used in subsequent calculations, as the cathodic part of the CV scan is better resolved in DMF but appears truncated and diminished in ACN solvent. All experimental redox values have an uncertainty of ±0.05 V.

2AP showed only a single set of redox peaks but exhibited irreversible electrochemistry. This has been observed for the native nucleic acids[40] as well. CV measurements were performed as a function of concentration (1−3 mM) to ascertain whether dimerization affected the shape of the CV curve. No concentration dependence was observed. Absorption spectra taken as a function of concentration (50 μM and 1 mM, data not shown) showed no spectral shifts or line shape changes, providing additional assurance that the doublet structure in the voltammograms was not due to dimers.

Calculated redox potentials of 2AP were obtained from the free energy changes for the formation of the radical cation or anion and subtracting from this the energy of neutral 2AP according to the method of Datta et al.[51] (see Table 2, columns 2, 4, 6, and 8). We have made the assumption that the sugar moiety does not affect the redox potential of 2AP significantly. The effect of different basis sets on the calculated redox potentials for 9-methyl-2AP was tested (see Table S.1 in the

TABLE 2: Comparison of 2AP Experimental ($E^{\circ EXP}_{REDOX}$) and Calculated ($E^{\circ C}_{REDOX}$) Redox Potentials[a]

ACN		DMF		ACN		DMF	
$E^{\circ EXP}_{OX}$	$E^{\circ C}_{OX}$	$E^{\circ EXP}_{OX}$	$E^{\circ C}_{OX}$	$E^{\circ EXP}_{RED}$	$E^{\circ C}_{RED}$	$E^{\circ EXP}_{RED}$	$E^{\circ C}_{RED}$
1.71	1.43	1.58	1.43	−2.13	−2.42	**−2.27**	−2.42

[a] The experimental potentials used are highlighted in bold and indicate the majority species and used for further analysis. The measurement error is estimated at ±0.05 V. All of the potentials reported here are referenced to the NHE.

Supporting Information). No significant improvement in the redox potentials was observed beyond the 6-31+G(d,p) level, even though the energies of the neutral, cation, or anion states varied as much as 100 kcal/mol (ΔE_{PCM}, see eq 2) between the most widely differing diffuse basis sets. This agreement can be ascribed to cancellation of errors when taking the energy difference of neutral and radical.

The free energy of each molecule was then calculated using the following equation:[51]

$$G^\circ = E_{PCM} + E_{Thermal} - TS \quad (2)$$

where E_{PCM} is the predicted single-point energy of the molecule in its lowest energy conformation inside the polarizable continuum described by the specified solvent, $E_{Thermal}$ is the thermal energy correction, S is the entropy of the molecule, and $T = 298.15$ K. The redox free energies, ΔG°_{OX} and ΔG°_{RED}, respectively, are given by

$$\Delta G^\circ_{OX} = G^\circ_{Cation} - G^\circ_{Neutral} = -nFE^{\circ FBA}_{OX} \quad (3)$$

$$\Delta G^\circ_{RED} = G^\circ_{Anion} - G^\circ_{Neutral} = -nFE^{\circ FBA}_{RED} \quad (4)$$

since $\Delta G^\circ = -nFE^\circ_{REDOX}$. The redox free energies were converted to redox potentials (against NHE) using eqs 5 and 6, where $\Delta G^\circ(H^+/(1/2H_2(g))) = -4.36$ eV when $n = 1$.

$$E^\circ_{OX}(V) = \frac{1}{n}\left[\Delta G^\circ_{OX} + \Delta G^\circ\left(\frac{H^+}{\frac{1}{2}H_2(g)}\right)\right] \quad (5)$$

$$E^\circ_{RED}(V) = \frac{1}{n}\left[\Delta G^\circ_{RED} - \Delta G^\circ\left(\frac{H^+}{\frac{1}{2}H_2(g)}\right)\right] \quad (6)$$

Table S.2 in the Supporting Information contains the parameters required to calculate the ground-state one electron redox potentials for 2AP in ACN and DMF using eqs 2−6. The calculated potentials are also recorded in Table 2, so a comparison with the experimental potentials can be made. The calculated oxidation potentials show virtually no variation with solvent, varying by a maximum of 0.2%. The reduction potentials showed a slightly larger variation of 1.1%. When water was used as the solvent, the redox potentials did not shift significantly (<100 mV, data not shown). ACN and DMF have very similar dielectric constants, so this agreement is not surprising given that the PCM model does not account for the specific interactions between solvent and solute.[47−49] The smaller than expected potential shift in water solvent highlights well-known deficiencies in the PCM model to account for hydrogen bonding.

TABLE 3: Excited-State Oxidation and Reduction Potentials of 2AP*[a]

	E_{00} (eV)				
	buffer	ACN	DMF	$E^{\circ 2AP^*}_{OX}$ (ACN)	$E^{\circ 2AP^*}_{RED}$ (DMF)
2AP*	3.67	3.73	3.71	−2.02	1.44

[a] E_{00} is the energy (in eV) at the intersection of normalized absorption and the fluorescence emission spectra as measured in 0.1 M potassium phosphate buffer, pH 7.0, ACN, or DMF. The estimated error is ±0.03 eV. The excited-state potentials for $E^{\circ 2AP^*}_{OX}$ and $E^{\circ 2AP^*}_{RED}$ are calculated using the E_{00} values for ACN and DMF, respectively.

2AP has one oxidation and reduction peak in both ACN and DMF. The measured oxidation potential, $E^{\circ EXP}_{OX}$, is 1.71 V in ACN and 1.58 V in DMF, compared to the calculated oxidation potential, $E^{\circ C}_{OX} = 1.43$ V, obtained for both solvents. The experimental reduction potentials in ACN and DMF are $E^{\circ\circ EXP}_{RED} = -2.13$ V and $E^{\circ EXP}_{RED} = -2.27$ V, respectively. These agree reasonably well with the calculated value, $E^{\circ C}_{RED} = -2.42$ V (for both DMF and ACN).

Excited-State Redox Potentials of the FBAs. The excited-state oxidation and reduction potentials, $E^{\circ FBA^*}_{OX}$ and $E^{\circ FBA^*}_{RED}$, can be calculated from the ground-state one electron oxidation and reduction potentials reported in Table 2 ($E^{\circ EXP}_{OX}$ and $E^{\circ EXP}_{RED}$) according to the following equations:

$$E^{\circ FBA^*}_{OX} = E^{\circ FBA}_{OX} - E_{00} \quad (7)$$

$$E^{\circ FBA^*}_{RED} = E^{\circ FBA}_{RED} + E_{00} \quad (8)$$

Table 3 lists these potentials, as well as the E_{00} energies of the FBAs. E_{00} is the energy difference between the ground state and first excited electronic state obtained from the intersection of the normalized absorption and fluorescence emission spectra[52] of 2AP in ACN or DMF for $E^{\circ FBA^*}_{OX}$ and $E^{\circ FBA^*}_{RED}$, respectively. It should be pointed out that the excited-state potentials are about 0.1 V larger if the aqueous E_{00} energy is used instead of the E_{00} obtained in the solvent used for the CV measurements. 2AP* gave an excited-state oxidation potential of −2.02 V. Its excited-state reduction potential is 1.44 V.

Free Energy of Electron Transfer (ΔG°_{ET}) for the Quenching of 2AP* by NMPs. The fluorescence quenching of 2AP* by the nucleic acid monophosphates through electron transfer can happen through two possible scenarios. 2AP* can reduce the ground-state NMP (nucleobase reduction or NBR), or it can be reduced by the NMP (nucleobase oxidation or NBO). Which of these two processes happens depends on the free energy change. The free energy change for the electron transfer step (ΔG°_{ET}, ET = NBO or NBR) for both NBO and NBR can be calculated using the classic Rehm−Weller equations:[39]

Nucleobase oxidation, NBO:

$$\Delta G^\circ_{NBO} = E^{\circ NMP}_{OX} - E^{\circ 2AP^*}_{RED} + \Delta G^\circ(\varepsilon) \quad (9)$$

TABLE 4: Oxidation/Reduction Potentials for the Native Bases for Comparison from the Work of Seidel et al.[40] and Crespo-Hernández et al.[53] [a]

NB	E°_{OX}(S)	E°_{OX}(CH)	E°_{RED}(S)	E°_{RED}(CH)
G	1.49	1.66	< -2.76	~ -3.00
A	1.96	1.83	-2.45	-2.71
C	2.14	1.96	-2.23	-2.56
dT	2.11	2.08	-2.14	-2.32

[a] E°_{OX}(S) and E°_{RED}(S) from ref 41; E°_{OX}(CH) and E°_{RED}(CH) from ref 54.

TABLE 5: Free Energies of Electron Transfer for 2AP (ΔG°_{ET}, in eV) Calculated from the Rehm−Weller Equation for the NBO (ΔG°_{NBO}) and the NBR (ΔG°_{NBR}) Schemes[a]

NB	ΔG°_{NBO}(S)	ΔG°_{NBR}(S)	ΔG°_{NBO}(CH)	ΔG°_{NBR}(CH)
G	-0.05	0.64	0.12	0.88
A	0.42	0.33	0.29	0.59
C	0.60	0.11	0.42	0.44
dT	0.57	0.02	0.54	0.20

[a] The free energies were calculated using data obtained in ACN or DMF for ΔG°_{NBO} or ΔG°_{NBR}, respectively (±0.06 eV). The free energies denoted "(S)" were calculated using columns 2 and 4 from Table 4. The free energies denoted "(CH)" were calculated using columns 3 and 5 from Table 4.

Nucleobase reduction, NBR:

$$\Delta G^{\circ}_{NBR} = E^{\circ 2AP^*}_{OX} - E^{\circ NMP}_{RED} + \Delta G^{\circ}(\varepsilon) \qquad (10)$$

where $E^{\circ 2AP^*}_{OX}$ and $E^{\circ 2AP^*}_{RED}$ are the excited-state oxidation and reduction potentials of 2AP*, respectively. $E^{\circ NMP}_{OX}$ and $E^{\circ NMP}_{RED}$ are the respective ground-state oxidation and reduction potentials of the nucleobase monophosphate. These potentials were obtained from the study of Seidel et al.[40] which involved a comprehensive evaluation of redox potentials measured using a variety of techniques. A more recent semiempirical study of the redox potentials of the native bases and 2-aminopurine by Crespo-Hernández et al.[53] (CH) presents a modified view of the Seidel study, and we explore the consequences of both these studies to PET in 2AP*:NMP complexes below. However, the CH potentials are specifically calculated as reversible redox potentials in ACN or DMF solvent. Both sets of redox potentials are tabulated in Table 4. The relative root-mean-square (rms) deviation between the two sets of oxidation potentials is a maximum of 11% for guanine with a average rms deviation of 7 ± 4%, while the reduction potentials differ at most by 15% (rms for cytosine) with a higher average rms deviation of about 11 ± 3%. The reduction potentials of CH are systematically more negative than those from Seidel's work.

The Born correction, $\Delta G^{\circ}(\varepsilon)$, is

$$\Delta G^{\circ}(\varepsilon) = \frac{e^2}{4\pi\varepsilon_o}\left[\left(\frac{1}{r_{ion}} - \frac{1}{r_{EC}}\right)\frac{1}{\varepsilon_W} - \frac{1}{r_{ion}\varepsilon_o}\right] \qquad (11)$$

which accounts for the interaction energy between the two radical ions formed after electron transfer and helps account for the solvent change from an organic solvent whose dielectric constant is ε_o, to that of a solvent of interest ε_W. In our case the organic solvent is either ACN or DMF and the solvent of interest is water. Using standard parameters for $r_{ion} = 3.0$ Å and $r_{EC} = 7.0$ Å, we obtain a $\Delta G^{\circ}(\varepsilon) = -0.093$ eV.[40]

The calculated ΔG°_{ET} values for NBO and NBR are listed in Table 5 using the two sets of redox potentials given in Table 4. Using Seidel's values, all ET free energies are positive with the exception of $\Delta G^{\circ}_{NBO} = -0.05$ eV for rGMP, suggesting that photoinduced electron transfer via NBO or NBR will not be spontaneous for dTMP, rCMP, and rAMP without a free energy contribution to solvation. This is discussed below. The free energies for NBR are, within experimental error, distinct from those for NBO, with the exception of rAMP. Thus, NBO will be a spontaneous or near-spontaneous process for rGMP, NBR for rCMP and dTMP, and either NBO or NBR for rAMP.

The CH redox values for the NBs were determined to reflect solvation in ACN or DMF and therefore are of particular interest here. All ET free energies are more positive than those obtained using Seidel's redox potentials. Again, rGMP represents the lowest free energy (for NBO) and therefore, given a sufficiently negative solvation free energy contribution, should undergo spontaneous electron transfer to 2AP*. dTMP has the next lowest free energy, this time for NBR, followed by rAMP via NBO and rCMP, which can undergo either NBO or NBR.

In either case, if the free energy contribution from water solvation, ΔG°_{W}, stabilizes the complex, the resulting decrease in ΔG°_{ET} could support spontaneous electron transfer quenching ($\Delta G^{\circ}_{ET} = \Delta G^{\circ}_{NBO\ or\ NBR} + \Delta G^{\circ}_{W}$), consistent with the measured k_q values that show that the quenching rates for these native bases are within 50% of the quenching rate for rGMP. The Born correction (~ -0.1 V) is not large enough to produce negative free energies for all NMPs in water. To address this issue, fluorescence quenching of 2AP* by adenosine and guanosine in DMF was tested. We were unable to use mononucleotides because they were insoluble in DMF. However, nucleosides were soluble in DMF up to at least 5 mM. No quenching was observed for either guanosine or adenosine (results not shown). Although it is not possible to directly compare these results in aqueous and nonaqueous solutions (because of the difference in quenchers), the results suggest that water significantly shifts the energetics of the quenching process and that the free energy for this solvation process is not accounted for in eqs 9−11.

An estimate of ΔG°_{W} for nucleobases, and a justification for obtaining the redox potentials of NBs in aprotic solvents, was laid out by Seidel et al.[40] They found that the redox values for the native bases obtained in aqueous solution were highly variable and technique dependent. CV measurements in aprotic polar solvents abolish proton-coupled electron transfer and other proton-driven chemical follow-up reactions, while retaining a polar dielectric environment similar to that of water. To compensate for the difference in solvation energies, they introduced a free energy shift, ΔG°_{W}, by adding this term into the energy argument of the Franck−Condon factor of the Marcus equation. They obtained ΔG°_{W} by fitting the quenching rate constants to the Marcus equation using the redox potentials of the NBs obtained in DMF. ΔG°_{W} was in the range of -0.5 to -0.9 eV. This averaged free energy aqueous solvation shift was argued to be consistent with the quenching data and with the redox potential results taken in different solvents by different techniques. The CH treatment does not include an estimate of ΔG°_{W} since it is concerned only with aprotic solvents.

The smallest shift necessary to allow for spontaneous NBO/NBR using Seidel's or redox potentials is about -0.33 eV (based on NBR for rAMP). This solvation shift produces spontaneous quenching of 2AP* by guanine through NBO, and cytosine, thymine, and adenine through NBR. (The free energies for adenine NBO and NBR are within the estimated error and the electron transfer direction may therefore not be distinguishable. We refer to this as NBX, where X = O or R.) Because of this mixed mechanism, the application of the Rehm−Weller formalism to determine ΔG°_{W} and λ is inappropriate. However, this

picture gives a thermodynamic ordering of $\{\Delta G^{\circ}_{NBO}(G) \sim \Delta G^{\circ}_{NBR}(dT), \Delta G^{\circ}_{NBR}(dT) \sim \Delta G^{\circ}_{NBR}(C)\} < \Delta G^{\circ}_{NBX}(A)$ in aqueous buffer, which is somewhat inconsistent with our k_q values since k_q for rGMP is larger than that for dTMP.

A slightly larger though still modest $\Delta G^{\circ}_{W} \sim -0.42$ eV is required to make PET quenching by NBO or NBR spontaneous based on the CH redox potentials. In this case, the purines undergo NBO and dTMP by NBR. Interestingly, cytosine can undergo either oxidation or reduction. The ordering based on these values would be $\{\Delta G^{\circ}_{NBO}(G) \sim \Delta G^{\circ}_{NBR}(dT), \Delta G^{\circ}_{NBR}(dT) \sim \Delta G^{\circ}_{NBO}(A)\} < \Delta G^{\circ}_{NBX}(C)$. This ordering leads to better agreement with k_q, although there is ambiguity in the ranking of quenching constants for dT and A due to experimental uncertainties. Interestingly, the two orderings lead to different predictions about whether NBO or NBR will be observed. To date, transient absorption data by groups cited in this work have not provided conclusive identification of NB radical ions reported. However, the semiempirical treatment of NB redox potentials of the Crespo-Hernández group seems to be supported by our kinetic and thermodynamic analysis here. Based on the accuracy of the free energy and k_q values (as opposed to their precision), we can rank the NBs in terms of quenching efficiency in the following base order: $rGMP_{NBO} > dTMP_{NBR} > rAMP_{NBO} > rCMP_{NBX}$. We recognize, however, that measurement precision would require an ordering of rGMP > (dTMP, rAMP, rCMP).

Discussion

2AP Excited-State Quenching. We have shown that all NMPs quench 2AP* in aqueous solution. The order of quenching we suggest is $rGMP_{NBO} > dTMP_{NBR} > rAMP_{NBO} > rCMP_{NBX}$. The CV and spectroscopic analysis suggest that the thermodynamic driving force is greatest for G and smallest for C: $\{\Delta G^{\circ}_{NBO}(G) \sim \Delta G^{\circ}_{NBR}(dT), \Delta G^{\circ}_{NBR}(dT) \sim \Delta G^{\circ}_{NBO}(A)\} < \Delta G^{\circ}_{NBX}(C)$.

Stern−Volmer quenching of 2AP* has been examined by several groups besides our own with varying results. The earliest account from Wierzchowski's group (1977)[32] for 2AP*:thymidine showed evidence of static complexation, with $K_S \sim 6\ M^{-1}$ and a dynamic quenching constant value of $K_d \sim 35\ M^{-1}$ at 21 °C compared to 2.2 M^{-1} and 19.4 M^{-1}, respectively, in this work. The quenching constant value of $k_q \sim 3 \times 10^9\ M^{-1}\ s^{-1}$ is about 50% larger than our value of $1.7 \times 10^9\ M^{-1}\ s^{-1}$ as it scales with the K_d constant. The agreement is reasonable, given that dTMP was used here compared to thymidine in the earlier study and the bulkier NMP will have a slower diffusion and perhaps more hindered complexation than the thymidine nucleoside. Another possibly significant difference is that Wierzchowski's results were obtained in unbuffered aqueous solutions using 1 mM 2AP with concentrations of thymidine ranging up to 260 mM.

In contrast, using dNTPs Kelley et al.[34] observed quenching with dGTP but not dATP (T and C were not mentioned). These results were obtained using 0.1 mM 2AP in 100 mM phosphate buffer, pH 7, at 20 °C. A linear S−V analysis was used and $k_q \sim 2.2 \times 10^9\ M^{-1}\ s^{-1}$ was obtained, which is about 13% lower than our value. This good agreement is not too surprising since we measured $K_S \sim 1.4\ M^{-1}$ for 2AP:rGMP, suggesting that quenching is mostly dynamic. We performed a control experiment using rGTP and rATP, but these also gave quenching to the same extent as the corresponding rNMPs shown in Table 1. It is possible that the 2′-OH group in the dGTP sugar plays a crucial role in tuning the free energy for the quenching process. However, the work of Seidel et al.[40] showed that 2′-deoxythymidine had almost the same quenching constant as 2′-hydroxyuridine (ribose form), suggesting that the quenching behavior is relatively independent of the sugar. Crespo-Hernández et al. also showed that the sugar has a modest effect on the redox potentials.[53] Stivers has shown that 2AP* in ss-DNA is quenched when flanked by several thymines on either side of the FBA.[54]

Further evidence that the other NBs could quench 2AP* was found by Rachofksy, Osman, and Ross. They obtained S−V quenching constants from steady-state and time-resolved fluorescence measurements for d2AP with rG, rA, rC, dT, ATP, and GTP[55] in 20−200 mM Tris:HCl buffer, 60 mM NaCl, 0.1 mM EDTA, pH 8. The quenching constants obtained from this work gives the ordering rA ∼ dT > rC > rG with d2AP* compared to our ordering of $rGMP_{NBO} > dTMP_{NBR} > rAMP_{NBO} > rCMP_{NBX}$ with 2AP free base. The actual values of k_q differ by less than 26% for all NBs with the exception of G, which is the best quencher in our study and the poorest in the Ross study. The reason for this may be due to the use of the nucleoside in the latter case and the monophosphate here. The ribonucleosides were not soluble enough to obtain K_S constants reliably; thus a fit to obtain this and the K_d constants would be difficult. The use of dT, GTP, and ATP did afford the Ross group with $K_S = 54\ M^{-1}$ for dT, and 32 M^{-1} for both purines, compared to 2.2 M^{-1} for dT and 1.4 and 5.0 M^{-1} for rGMP and rAMP here. The difference is striking and may be due to differences in the buffer systems (including the use of EDTA). However, another possibility is that the titrations were performed to a significantly higher NB concentration than we employed, ∼300 mM compared to 50 mM, respectively. It may be that higher aggregates account for the much higher K_S values seen by the Ross group. In summary, the significant deviation in ordering is difficult to rationalize. However, rGMP showed the most negative ΔG°_{ET} (for NBO) of any NB in this study, and this suggests that it should be the most efficient quencher. Other studies cited herein appear to support this conclusion.

Our results agree with the work by Amerongen et al.,[30,31] who observed quenching in 2AP-containing dinucleotides (presumably deoxy) using femtosecond transient absorption. They showed that the magnitude of quenching occurs in the order dGTP > dTTP > dATP ∼ dCTP. An important difference in the systems studied is that the dinucleotides have a much more well-defined, if constrained, interaction geometry than free bases colliding in solvent. This difference would be invisible in our measurements of k_q since we are not able to resolve any kinetics faster than the diffusion rate.

2AP Redox Potentials. We obtained 1.71 V for the ground-state oxidation potential of 2AP in ACN. This value should shift to lower potentials in aqueous medium. Yao and Musha reported a value of 0.98 V for 2AP in aqueous solution (pH 7).[37] Examination of the redox potentials reported for the various native nucleic acids shows a minimum shift of about 700 mV in going from a nonaqueous to an aqueous environment.[40] Thus our 2AP value is in good agreement with Yao and Musha.

Crespo-Hernández et al. calculated the oxidation potential of d2AP = 1.86 V (in DMF or ACN). This is within 9% of our experimental result but significantly higher than our DFT calculation. Given the semiempirical nature of the study, it is not surprising that the adjusted DFT calculation of CH would produce better agreement with this experiment. Interestingly, though, they predict that d2AP* will reduce dGuo and dAdo and oxidize dCyd and dThd in DMF or ACN. This was not seen experimentally in our work (vide supra) for 2AP free base with either rA or rG in DMF. However, as described above, the $\Delta G^{\circ}_{ET}(C)$ found here are all positive and therefore we do not expect 2AP* quenching in DMF by either NBO or NBR.

The excited-state reduction potential of $E^{\circ 2AP^*}_{RED} = 1.44$ V in DMF is very close to the aqueous value reported by Fiebig[29] and Barton et al.[34] of 1.5 V. On closer examination this agreement may be fortuitous. The $E^{\circ 2AP^*}_{RED}$ obtained by Fiebig was based on a fit of k_{ET} obtained from transient absorption of 2AP:nucleobase complexes in aqueous buffer. We cannot ignore the potential shift in going from DMF to water, which must be several tenths of a volt.

A possible resolution of the two values may be had from an examination of one of the assumptions in fitting k_{ET} from the ultrafast experiments. The reorganization energy for these PET reactions was set to $\lambda_0 = 1.2$ eV assuming spherical reactants and a net zero initial dipole moment of the donor−acceptor pair before electron transfer.[56] However, molecules which have large permanent ground state dipole moments will undergo significant alignment in the formation of the (transient) encounter complex, which should, in turn, leading to a decrease in λ_0. Dipole−dipole interactions lead to a lowest energy "head-to-tail" geometry.[57] This may be true of 2AP and the NMPs, in spite of significant dielectric screening of the dipoles in polar (aqueous) solvent. Whether this geometry leads to highly efficient PET remains to be determined.

Assuming this is the average geometry of the encounter complex, the net change in dipole moment due to electron transfer ($D-A \rightarrow D^{\bullet+}-A^{\bullet-}$) should be smaller than predicted if the reactants had the assumed zero dipole moment. Eberson, for example, has tabulated many cases where $\lambda_0 \ll 1$ eV.[58] We have seen this to be the case for FBAs based on pteridones or pteridones complexed with NMPs where PET is involved.[41] In these systems $\lambda_0 < 0.2$ eV. This recalibration of reorganization energies for FBAs with nonzero dipole moments could impact our understanding of 2-aminopurine PET. We were not able to determine the ET free energy for 2AP because of its mixed NBO/NBR behavior. However, this study suggests that $E^{\circ 2AP^*}_{RED}$ could be significantly higher than previously thought.

Finally, the quenching rate constants obtained here are likely to reflect the geometry of the encounter complex, while quenching in oligonucleotides most likely involves an entirely different geometry of the reactants. Nonetheless, the excited-state redox potentials for 2AP* measured in this study should be applicable to elucidating the spontaneity of PET involving 2AP* and the native bases in ss- and ds-DNA.

Conclusions

To our knowledge, we have presented the first measurements of one electron oxidation and reduction potentials of 2AP in aprotic organic solvents and the first determination of the 2AP reduction potential in any solvent using cyclic voltammetry. The corresponding excited-state redox potentials were obtained. These excited-state potentials were used in the Rehm−Weller equation to calculate free energies of electron transfer for both nucleobase oxidation and reduction by 2AP*. Taking into account the decrease in free energy in going from organic to aqueous solution, these values suggest that 2AP* oxidizes rGMP and rAMP but reduces dTMP. The electron transfer direction in PET involving 2AP* with rCMP could occur by either nucleobase oxidation or reduction based on the near equivalence of ΔG°_{NBO} and ΔG°_{NBR}.

Acknowledgment. We wish to thank Dr. Eric Borguet, Department of Chemistry, Temple University, for access to his potentiostat and for useful discussions. M.N. would like to thank Mr. Venkat Velvadapu of Dr. Rodrigo Andrade's research group, Department of Chemistry, Temple University. M.N. and R.J.S. would like to thank Dr. Vincent Rotello at the University of Massachusetts at Amherst and Dr. Anthony Addison at Drexel University for their valuable input on the CV results. Drs. Torsten Fiebig (Northwestern University) and Vladimir Shafirovich (NYU) provided useful discussions about the redox potentials of 2AP. M.N. was supported, in part, by NSF Grant CHE-0847855. This research was supported in part by Grant MCB080057P from the Pittsburgh Supercomputer Center, supported by several federal agencies, the Commonwealth of Pennsylvania, and private industry.

Note Added after ASAP Publication. This paper was published ASAP on July 27, 2010. Wording was changed in the Results section. The revised paper was reposted on August 12, 2010.

Supporting Information Available: Complete ref 45; tables of calculated one electron oxidation/reduction potentials of 9-methyl-2AP. This material is available free of charge via the Internet at http://pubs.acs.org/.

References and Notes

(1) Bloomfield, V. A.; Crothers, D. M.; Tinoco, I. J. *Physical chemistry of nucleic acids*; Harper and Row: New York, 1974.

(2) Santalucia, J., Jr. The use of spectroscopic techniques in the study of DNA stability. In *Spectrophotometry and Spectrofluorimetry*, 2nd ed.; Oxford University Press: New York, 2000; pp 329−356.

(3) Peon, J.; Zewail, A. H. DNA/RNA nucleotides and nucleosides: direct measurement of excited-state lifetimes by femto-second fluorescence up-conversion. *Chem. Phys. Lett.* **2001**, *348* (3,4), 255–262.

(4) Gustavsson, T.; Sharonov, A.; Markovitsi, D. Thymine, thymidine and thymidine 5′-monophosphate studied by femtosecond fluorescence upconversion spectroscopy. *Chem. Phys. Lett.* **2002**, *351* (3,4), 195–200.

(5) Gustavsson, T.; Sharonov, A.; Onidas, D.; Markovitsi, D. Adenine, deoxyadenosine and deoxyadenosine 5′-monophosphate studied by femtosecond fluorescence upconversion spectroscopy. *Chem. Phys. Lett.* **2002**, *356* (1,2), 49–54.

(6) Cohen, B.; Hare, P. M.; Kohler, B. Ultrafast Excited-State Dynamics of Adenine and Monomethylated Adenines in Solution: Implications for the Nonradiative Decay Mechanism. *J. Am. Chem. Soc.* **2003**, *125* (44), 13594–13601.

(7) Crespo-Hernandez, C. E.; Cohen, B.; Hare, P. M.; Kohler, B. Ultrafast Excited-State Dynamics in Nucleic Acids. *Chem. Rev.* **2004**, *104* (4), 1977–2019.

(8) Reuther, A.; Nikogosyan, D. N.; Laubereau, A. Primary Photochemical Processes in Thymine in Concentrated Aqueous Solution Studied by Femtosecond UV Spectroscopy. *J. Phys. Chem.* **1996**, *100* (13), 5570–5577.

(9) Yarkony, D. R. Conical Intersections: The New Conventional Wisdom. *J. Phys. Chem. A* **2001**, *105* (26), 6277–6293.

(10) Matsika, S. Conical intersections in molecular systems. *Rev. Comput. Chem.* **2007**, *23*, 83–124.

(11) Domcke, W.; Yarkony, D. R.; Koppel, H. *Conical Intersections: Electronic Structure, Dynamics, and Spectroscopy*; World Scientific Publishing Co.: Hackensack, NJ, 2004.

(12) Ward, D. C.; Reich, E.; Stryer, L. Fluorescence Studies of Nucleotides and Polynucleotides. *J. Biol. Chem.* **1969**, *244* (5), 1228–1237.

(13) Nordlund, T. M.; Andersson, S.; Nilsson, L.; Rigler, R.; Graeslund, A.; McLaughlin, L. W. Structure and dynamics of a fluorescent DNA oligomer containing the EcoRI recognition sequence: fluorescence, molecular dynamics, and NMR studies. *Biochemistry* **1989**, *28* (23), 9095–9103.

(14) Evans, K.; Xu, D.; Kim, Y.; Nordlund, T. M. 2-Aminopurine optical spectra: solvent, pentose ring, and DNA helix melting dependence. *J. Fluoresc.* **1992**, *2* (4), 209–216.

(15) Nordlund, T. M.; Xu, D.; Evans, K. O. Excitation energy transfer in DNA: Duplex melting and transfer from normal bases to 2-aminopurine. *Biochemistry* **1993**, *32* (45), 12090–12095.

(16) Guest, C. R.; Hochstrasser, R. A.; Sowers, L. C.; Millar, D. P. Dynamics of mismatched base pairs in DNA. *Biochemistry* **1991**, *30* (13), 3271–3279.

(17) Xu, D.; Evans, K. O.; Nordlund, T. M. Melting and Premelting Transitions of an Oligomer Measured by DNA Base Fluorescence and Absorption. *Biochemistry* **1994**, *33* (32), 9592–9529.

(18) Law, S. M.; Eritja, R.; Goodman, M. F.; Breslauer, K. J. Spectroscopic and Calorimetric Characterizations of DNA Duplexes Containing 2-Aminopurine. *Biochemistry* **1996**, *35* (38), 12329–12337.

(19) Bloom, L. B.; Otto, M. R.; Eritja, R.; Reha-Krantz, L. J.; Goodman, M. F.; Beechem, J. M. Pre-Steady-State Kinetic Analysis of Sequence-Dependent Nucleotide Excision by the 3′-Exonuclease Activity of Bacteriophage T4 DNA Polymerase. *Biochemistry* **1994**, *33* (24), 7576–7586.

(20) Raney, K. D.; Sowers, L. C.; Millar, D. P.; Benkovic, S. J. A fluorescence-based assay for monitoring helicase activity. *Proc. Natl. Acad. Sci. U.S.A.* **1994**, *91* (14), 6644–6648.

(21) Frey, M. W.; Sowers, L. C.; Millar, D. P.; Benkovic, S. J. The nucleotide analog 2-aminopurine as a spectroscopic probe of nucleotide incorporation by the Klenow fragment of Escherichia coli polymerase I and bacteriophage T4 DNA polymerase. *Biochemistry* **1995**, *34* (28), 9185–9192.

(22) Allan, B. W.; Reich, N. O. Targeted base stacking disruption by the EcoRI DNA methyltransferase. *Biochemistry* **1996**, *35* (47), 14757–14762.

(23) McCullough, A. K.; Dodson, M. L.; Scharer, O. D.; Lloyd, R. S. The role of base flipping in damage recognition and catalysis by T4 endonuclease V. *J. Biol. Chem.* **1997**, *272* (43), 27210–27217.

(24) Allan, B. W.; Beechem, J. M.; Lindstrom, W. M.; Reich, N. O. Direct real time observation of base flipping by the EcoRI DNA methyltransferase. *J. Biol. Chem.* **1998**, *273* (4), 2368–2373.

(25) Holz, B.; Klimasauskas, S.; Serva, S.; Weinhold, E. 2-Aminopurine as a fluorescent probe for DNA base flipping by methyltransferases. *Nucleic Acids Res.* **1998**, *26* (4), 1076–1083.

(26) Stivers, J. T.; Pankiewicz, K. W.; Watanabe, K. A. Kinetic Mechanism of Damage Site Recognition and Uracil Flipping by Escherichia coli Uracil DNA Glycosylase. *Biochemistry* **1999**, *38* (3), 952–963.

(27) Christine, K. S.; MacFarlane, A. W., IV; Yang, K.; Stanley, R. J. Cyclobutylpyrimidine Dimer Base Flipping by DNA Photolyase. *J. Biol. Chem.* **2002**, *277* (41), 38339–38344.

(28) Yang, K.; Stanley, R. J. Differential Distortion of Substrate Occurs When It Binds to DNA Photolyase: A 2-Aminopurine Study. *Biochemistry* **2006**, *45* (37), 11239–11245.

(29) Fiebig, T.; Wan, C.; Zewail, A. H. Femtosecond charge transfer dynamics of a modified DNA base: 2-aminopurine in complexes with nucleotides. *ChemPhysChem* **2002**, *3* (9), 781–788.

(30) Larsen, O. F. A.; van Stokkum, I. H. M.; de Weerd, F. L.; Vengris, M.; Aravindakumar, C. T.; van Grondelle, R.; Geacintov, N. E.; van Amerongen, H. Ultrafast transient-absorption and steady-state fluorescence measurements on 2-aminopurine substituted dinucleotides and 2-aminopurine substituted DNA duplexes. *Phys. Chem. Chem. Phys.* **2004**, *6* (1), 154–160.

(31) Somsen, O. J. G.; Van Hoek, A.; Van Amerongen, H. Fluorescence quenching of 2-aminopurine in dinucleotides. *Chem. Phys. Lett.* **2005**, *402* (1−3), 61–65.

(32) Bierzynski, A.; Kozlowska, H.; Wierzchowski, K. L. Investigations on purine and pyrimidine bases stacking associations in aqueous solutions by the fluorescence quenching method. II. Heteroassociation between 2-aminopurine and thymidine. *Biophys. Chem.* **1977**, *6* (3), 223–229.

(33) Bierzynski, A.; Kozlowska, H.; Wierzchowski, K. L. Investigation on purine and pyrimidine bases stacking associations in aqueous solutions by the fluorescence quenching method. I. Autoassociation of 2-aminopurine. *Biophys. Chem.* **1977**, *6* (3), 213–222.

(34) Kelley, S. O.; Barton, J. K. Electron transfer between bases in double helical DNA. *Science (Washington, D.C.)* **1999**, *283* (5400), 375–381.

(35) Reynisson, J.; Steenken, S. One-electron reduction of 2-aminopurine in the aqueous phase. A DFT and pulse radiolysis study. *Phys. Chem. Chem. Phys.* **2005**, *7* (4), 659–665.

(36) Marcus, R. A.; Sutin, N. Electron transfers in chemistry and biology. *Biochim. Biophys. Acta* **1985**, *811* (3), 265–322.

(37) Yao, T.; Musha, S. The electrochemical oxidation of aminopurines and their hydroxy derivatives at the glassy carbon electrode. *Bull. Chem. Soc. Jpn.* **1979**, *52* (8), 2307–11.

(38) Lakowicz, J. R. *Principles of Fluorescence Spectroscopy*, 3rd ed.; Springer: New York, 2006.

(39) Rehm, D.; Weller, A. Kinetics of Fluorescence Quenching by Electron and H-Atom Transfer. *Isr. J. Chem.* **1970**, *8*, 259–271.

(40) Seidel, C. A. M.; Schulz, A.; Sauer, M. H. M. Nucleobase-Specific Quenching of Fluorescent Dyes. 1. Nucleobase One-Electron Redox Potentials and Their Correlation with Static and Dynamic Quenching Efficiencies. *J. Phys. Chem.* **1996**, *100* (13), 5541–5553.

(41) Narayanan, M.; Kodali, G.; Xing, Y.; Hawkins, M. E.; Stanley, R. J. Differential Fluorescence Quenching of Fluorescent Nucleic Acid Base Analogues by Native Nucleic Acid Monophosphates. *J. Phys. Chem. B* **2010**, *114* (17), 5953–5963.

(42) Cavaluzzi, M. J.; Borer, P. N. Revised UV extinction coefficients for nucleoside-5′-monophosphates and unpaired DNA and RNA. *Nucleic Acids Res.* **2004**, *32* (1), 1–9.

(43) Smagowicz, J.; Wierzchowski, K. L. Lowest excited states of 2-aminopurine. *J. Lumin.* **1974**, *8* (3), 210–232.

(44) Pavlishchuk, V. V.; Addison, A. W. Conversion constants for redox potentials measured versus different reference electrodes in acetonitrile solutions at 25°C. *Inorg. Chim. Acta* **2000**, *298*, 97–102.

(45) Frisch, M. J.; Trucks, G. W.; Schlegel, H. B.; Scuseria, G. E.; Robb, M. A.; Cheeseman, J. R.; Montgomery, J. A., Jr.; Vreven, T.; Kudin, N. K.; Burant, J. C.; Millam, J. M.; Iyengar, S. S.; Tomasi, J.; Barone, V.; Mennucci, B.; Cossi, M.; Scalmani, G.; Rega, N.; Petersson, G. A.; Nakatsuji, H.; Hada, M.; Ehara, M.; Toyota, K.; Fukuda, R.; Hasegawa, J.; Ishida, M.; Nakajima, T.; Honda, Y.; Kitao, O.; Nakai, H.; Klene, M.; Li, X.; Knox, J. E.; Hratchian, H. P.; Cross, J. B.; Adamo, C.; Jaramillo, J.; Gomperts, R.; Stratmann, R. E.; Yazyev, O.; Austin, A. J.; Cammi, R.; Pomelli, C.; Ochterski, J. W.; Ayala, P. Y.; Morokuma, K.; Voth, G. A.; Salvador, P.; Dannenberg, J. J.; Zakrzewski, V. G.; Dapprich, S.; Daniels, A. D.; Strain, M. C.; Farkas, O.; Malick, D. K.; Rabuck, A. D.; Raghavachari, K.; Foresman, J. B.; Ortiz, J. V.; Cui, Q.; Baboul, A. G.; Clifford, S.; Cioslowski, J.; Stefanov, B. B.; Liu, G.; Liashenko, A.; Piskorz, P.; Komaromi, I.; Martin, R. L.; Fox, D. J.; Keith, T.; Al-Laham, M. A.; Peng, C. Y.; Nanayakkara, A.; Challacombe, M.; Gill, P. M. W.; Johnson, B.; Chen, W.; Wong, M. W.; Gonzalez, C.; Pople, J. A. *Gaussian 03*, revision A.1; Gaussian, Inc.: Pittsburgh, PA, 2003.

(46) Böes, E. S.; Livotto, P. R.; Stassen, H. Solvation of monovalent anions in acetonitrile and N, N-dimethylformamide: Parameterization of the IEF-PCM model. *Chem. Phys.* **2006**, *331*, 142–158.

(47) Miertus, S.; Scrocco, E.; Tomasi, J. Electrostatic interaction of a solute with a continuum. A direct utilizaion of AB initio molecular potentials for the prevision of solvent effects. *Chem. Phys.* **1981**, *55* (1), 117–129.

(48) Miertus, S.; Tomasi, J. Approximate evaluations of the electrostatic free energy and internal energy changes in solution processes. *Chem. Phys.* **1982**, *65* (2), 239–245.

(49) Pascual-Ahuir, J. L.; Silla, E.; Tomasi, J.; Bonaccorsi, R. Electrostatic interaction of a solute with a continuum. Improved description of the cavity and of the surface cavity bound charge distribution. *J. Comput. Chem.* **2004**, *8* (6), 778–787.

(50) Bharill, S.; Sarkar, P.; Ballin, J. D.; Gryczynski, I.; Wilson, G. M.; Gryczynski, Z. Fluorescence intensity decays of 2-aminopurine solutions: Lifetime distribution approach. *Anal. Biochem.* **2008**, *377* (2), 141–149.

(51) Pandey, A.; Datta, S. N. Theoretical Determination of Standard Oxidation and Reduction Potentials of Chlorophyll-a in Acetonitrile. *J. Phys. Chem. B* **2005**, *109* (18), 9066–9072.

(52) Kavarnos, G. J. *Fundamentals of photoinduced electron transfer*; VCH Publishers, Inc.: New York, 1993.

(53) Crespo-Hernández, C. E.; Close, D. M.; Gorb, L.; Leszczynski, J. Determination of redox potentials for the Watson-Crick base pairs, DNA nucleosides, and relevant nucleoside analogues. *J. Phys. Chem. B* **2007**, *111* (19), 5386–5395.

(54) Stivers, J. T. 2-Aminopurine fluorescence studies of base stacking interactions at abasic sites in DNA: metal-ion and base sequence effects. *Nucleic Acids Res.* **1998**, *26* (16), 3837–3844.

(55) Rachofsky, E. L.; Osman, R.; Ross, J. B. A. Probing Structure and Dynamics of DNA with 2-Aminopurine: Effects of Local Environment on Fluorescence. *Biochemistry* **2001**, *40* (4), 946–956.

(56) Sutin, N. Theory of electron transfer reactions: insights and hindsights. *Prog. Inorg. Chem.* **1983**, *30*, 441–498.

(57) Parsons, W. W. *Modern Optical Spectroscopy*; Springer: Berlin, Heidelberg, 2007.

(58) Eberson, L. Electron-transfer reactions in organic chemistry. *Adv. Phys. Org. Chem.* **1982**, *18*, 79–185.

(59) Holmen, A.; Norden, B.; Albinsson, B. Electronic transition moments of 2-aminopurine. *J. Am. Chem. Soc.* **1997**, *119* (13), 3114–3121.

JP102355V